JCI insight

Eosinophils downregulate lung alloimmunity by decreasing TCR signal transduction

Oscar Okwudiri Onyema, … , Elizabeth A. Jacobsen, Alexander Sasha Krupnick

JCI Insight. 2019;4(11):e128241. https://doi.org/10.1172/jci.insight.128241.

Research Article | Immunology | Transplantation

Despite the accepted notion that granulocytes play a universally destructive role in organ and tissue grafts, it has been recently described that eosinophils can facilitate immunosuppression-mediated acceptance of murine lung allografts. The mechanism of eosinophil-mediated tolerance, or their role in regulating alloimmune responses in the absence of immunosuppression, remains unknown. Using lung transplants in a fully MHC-mismatched BALB/c ($H2^d$) to C57BL/6 ($H2^b$) strain combination, we demonstrate that eosinophils downregulate T cell–mediated immune responses and play a tolerogenic role even in the absence of immunosuppression. We further show that such downregulation depends on PD-L1/PD-1–mediated synapse formation between eosinophils and T cells. We also demonstrate that eosinophils suppress T lymphocyte responses through the inhibition of T cell receptor/CD3 (TCR/CD3) subunit association and signal transduction in an inducible NOS–dependent manner. Increasing local eosinophil concentration, through administration of intratracheal eotaxin and IL-5, can ameliorate alloimmune responses in the lung allograft. Thus, our data indicate that eosinophil mobilization may be utilized as a novel means of lung allograft–specific immunosuppression.

Find the latest version:

http://jci.me/128241/pdf



JCI insight

RESEARCH ARTICLE

Eosinophils downregulate lung alloimmunity by decreasing TCR signal transduction

Oscar Okwudiri Onyema,[1] Yizhan Guo,[1] Bayan Mahgoub,[1] Qing Wang,[1] Amir Manafi,[1] Zhongcheng Mei,[1] Anirban Banerjee,[1] Dongge Li,[1] Mark H. Stoler,[2] Melissa T. Zaidi,[3] Adam G. Schrum,[3] Daniel Kreisel,[4] Andrew E. Gelman,[4] Elizabeth A. Jacobsen,[5] and Alexander Sasha Krupnick[1]

[1]Department of Surgery, Carter Center for Immunology, and [2]Department of Pathology, University of Virginia, Charlottesville, Virginia, USA. [3]Molecular Microbiology and Immunology, Surgery, Bioengineering, University of Missouri, Columbia, Missouri, USA. [4]Department of Surgery, Washington University, St. Louis, Missouri, USA. [5]Division of Allergy, Asthma and Clinical Immunology, Mayo Clinic, Scottsdale, Arizona, USA.

Despite the accepted notion that granulocytes play a universally destructive role in organ and tissue grafts, it has been recently described that eosinophils can facilitate immunosuppression-mediated acceptance of murine lung allografts. The mechanism of eosinophil-mediated tolerance, or their role in regulating alloimmune responses in the absence of immunosuppression, remains unknown. Using lung transplants in a fully MHC-mismatched BALB/c ($H2^d$) to C57BL/6 ($H2^b$) strain combination, we demonstrate that eosinophils downregulate T cell–mediated immune responses and play a tolerogenic role even in the absence of immunosuppression. We further show that such downregulation depends on PD-L1/PD-1–mediated synapse formation between eosinophils and T cells. We also demonstrate that eosinophils suppress T lymphocyte responses through the inhibition of T cell receptor/CD3 (TCR/CD3) subunit association and signal transduction in an inducible NOS–dependent manner. Increasing local eosinophil concentration, through administration of intratracheal eotaxin and IL-5, can ameliorate alloimmune responses in the lung allograft. Thus, our data indicate that eosinophil mobilization may be utilized as a novel means of lung allograft–specific immunosuppression.

Introduction

Lung grafts have the worst overall survival of all solid organs (1). A complex and unique immunoregulatory network, that differs significantly from other organ grafts, is at least partially responsible for such poor long-term outcomes. Clinically accepted immunosuppression regimens, that globally downregulate or even temporarily ablate the adaptive immune response, result in acceptable long-term survival of heart and kidney grafts but yield close to a 50% lung allograft loss 5 years after engraftment (2). We and others have suggested that unique immunoregulatory pathways that contribute to acceptance of this mucosal barrier organ may require a different strategy for long-term graft survival (3, 4). For example, depletion of $CD8^+$ T cells as well as other proinflammatory cells contributes to the acceptance of most transplanted organs but prevents lung allograft acceptance (5, 6).

Along those lines, we have recently demonstrated that eosinophils, a granulocytic population long considered deleterious for long-term graft function, play a critical role in costimulatory blockade–mediated (CSB-mediated) induction of lung allograft tolerance (7). The role of this cell population in the absence of CSB or its mechanism(s) of immunosuppression remain unknown. Here we demonstrate that eosinophils play a unique role in the downregulation of the lung alloimmune response even in the absence of traditional or CSB-mediated immunosuppression. Thus, unlike the case for other solid organs, eosinophils play an exclusive and solely tolerogenic role in the lung allograft (8). Mechanistically, we demonstrate that Th1-polarized eosinophils inhibit $CD8^+$ T cell proliferation by interfering with T cell receptor/CD3 (TCR/CD3) subunit association and signal transduction in an inducible NOS–dependent (iNOS-dependent) manner. We further show that PD-L1–dependent eosinophil–T cell contact is critical for eosinophil suppressive function.

Authorship note: OOO and YG contributed equally to this work.

Conflict of interest: ASK is the Founder, Scientific Director, and Board Member of Courier Therapeutics (www.couriertherapeutics.com).

Copyright: © 2019 American Society for Clinical Investigation

Submitted: February 18, 2019
Accepted: April 23, 2019
Published: June 6, 2019.

Reference information: *JCI Insight*. 2019;4(11):e128241. https://doi.org/10.1172/jci.insight.128241.

Results

E1-polarized eosinophils accumulate in tolerant and rejecting lung allografts. It has been demonstrated by us as well as others that eosinophils may alter their phenotype and function based on the local environment (7, 9, 10). Since costimulation plays a critical role in T cell cytokine production and environmental polarization (11, 12), we examined the possibility that eosinophils may lose their tolerogenic properties in the absence of CSB immunosuppression. Cytokine expression was examined in BALB/c ($H2^d$) lung allografts transplanted into fully MHC-mismatched C57BL/6 (B6) ($H2^b$) recipient mice. In the absence of immunosuppression, lung allografts had higher levels of Th1-polarizing cytokines IFN-γ and TNF-α than did CSB-treated accepting lung grafts (Figure 1A). Limited amounts of Th2-polarizing cytokines IL-4, IL-13, IL-33, and GM-CSF were evident in lung allografts treated with or without CSB immunosuppression (Supplemental Figure 1A; supplemental material available online with this article; https://doi.org/10.1172/jci.insight.128241DS1). We next evaluated lung-resident eosinophils from both CSB-treated and nonimmunosuppressed grafts. Based on a previously identified eosinophil polarization phenotype (7), we noted higher levels of Th1-defining (or E1-defining) features, such as CXCL9, CXCL10, CXCL11, and iNOS in eosinophils isolated from rejecting compared with CSB-treated lung allografts (Figure 1A). In no group was Th2 (or E2) polarization of eosinophils detected (Supplemental Figure 1A). Flow cytometric characterization demonstrated an absence of MHC II and costimulatory molecules such as CD80, CD86, and CD40. However, there were high levels of recipient-derived MHC I ($H2K^b$), PD-L1, and CD101 on lung-resident eosinophils in the absence of CSB (Figure 1B). Notably, we did not detect BALB/c-derived $H2^d$-MHC on graft-resident eosinophils, indicating a lack of "cross-dressing" or antigen swapping for donor derived–antigens (ref. 13 and Supplemental Figure 1B). Thus, while eosinophils from rejecting lungs resembled those from accepting lungs in some aspects, we did observe some differences. It is thus possible that in the absence of immunosuppression, eosinophils may contribute to graft rejection rather than acceptance, specifically because CD101 expression has been previously associated with an inflammatory eosinophil subtype (14).

In order to evaluate this directly, we conditionally depleted eosinophils from B6 iPHIL mice, in which the diphtheria toxin (DT) receptor is expressed under the control of the eosinophil peroxidase promoter (Supplemental Figure 1C and ref. 15). DT-treated mice or saline-injected controls were challenged with a BALB/c lung allograft in the absence of immunosuppression. Surprisingly, mice depleted of eosinophils had higher grades of rejection (Figure 1C), increased numbers of lung-resident T lymphocytes, increased rates of T cell proliferation, and increased effector cell differentiation by day 4 after engraftment (Figure 1D). These patterns of T lymphocyte activation and infiltration were especially prominent for $CD8^+$ T cells. $CD4^+$ T cell proliferation did increase slightly in the absence of eosinophils, but the relative proportion of $CD44^{hi}CD62L^{lo}$ effector cells did not change (Figure 1D).

To further characterize eosinophil-mediated effects on $CD8^+$ T cells, we transcript profiled lung allograft–resident $CD8^+$ T cells in eosinophil-sufficient or eosinophil-depleted mice. Principal component analysis (PCA) demonstrated that $CD8^+$ T cells from eosinophil-sufficient or -deficient mice differed substantially (Figure 2A). Gene expression analysis demonstrated an upregulation of 2956 and downregulation of 2360 genes in the absence of eosinophils (Supplemental Figure 2A). Using unbiased hierarchical gene ontology analysis to cluster the 5316 differentially expressed genes, we noted significant upregulation of the inflammatory response, immune system processing, and cell proliferation clusters as 3 of the top 4 clusters among the 27 gene ontology groups that differ substantially between lung-resident $CD8^+$ T cells in eosinophil-depleted and eosinophil-sufficient mice (Figure 2B and Supplemental Figure 2B). Taken together, our results show that eosinophils play a unique and unequivocal role in the downregulation of $CD8^+$ T cell–mediated alloimmune responses in the lung allograft. However, mechanistic aspects of $CD8^+$ T cell suppression remain unknown.

Eosinophils suppress T cell responses in a dose-, contact-, and iNOS-dependent manner. In order to further define the mechanism(s) of eosinophil-mediated immunosuppression, we took a reductionist approach and cocultured increasing ratios of E1-polarized eosinophils with B6 T cells in the presence of anti–CD3/CD28 polyclonal stimulation for a total of 5 days in vitro. Consistent with our observations in vivo, eosinophils inhibited both proliferation as well as effector differentiation of $CD8^+$ T cells in a dose-dependent manner, even in the absence of professional antigen-presenting cells (APCs) (Figure 3A). A similar, but less pronounced, degree of inhibition was observed for $CD4^+$ T cells (Supplemental Figure 3A). We next set out to define in more detail factors that control eosinophil-mediated T cell regulation. We specifically focused on iNOS, based on its upregulation in the lung graft (Figure 1A and ref. 7), as well as physical contact of

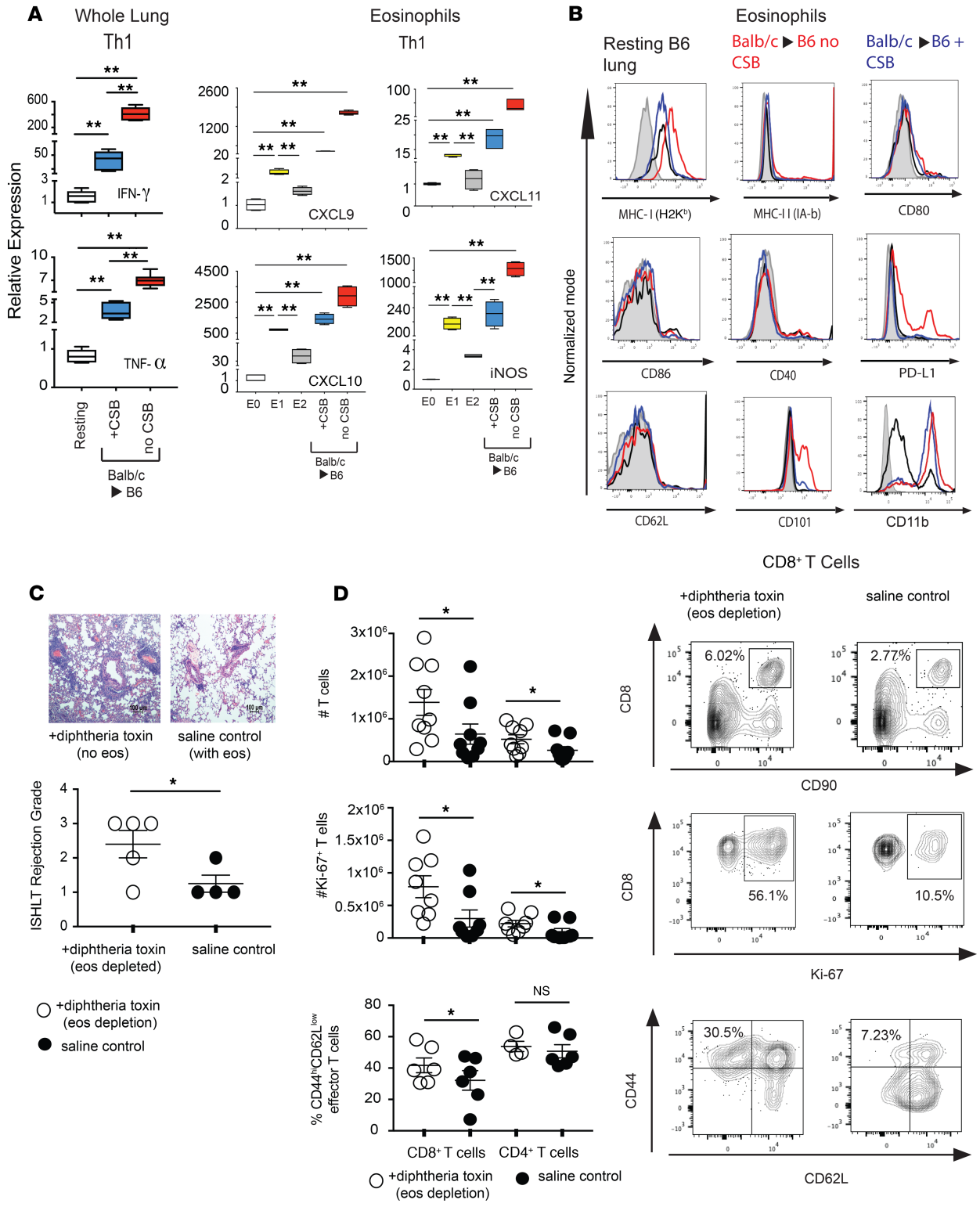


Figure 1. Th1 polarization of the lung allograft. (**A**) Seven days after transplantation of BALB/c lung allograft to B6 recipient with or without CSB immunosuppression, the whole lung allograft (left) or flow cytometrically sorted lung-resident eosinophils (right) were phenotyped for Th1 or Th2 polarization using established markers. Comparison was made to E0 resting blood-resident eosinophils (white) or eosinophils polarized to the E1 (Th1) phenotype by overnight exposure to IFN-γ and TNF-α (yellow) or E2 (Th2) phenotype by overnight exposure to IL-33, IL-4, and GM-CSF (gray). Representative of 4 to 6 transplants per group, with Th2 analysis presented in Supplemental Figure 1. (**B**) Flow cytometric analysis of lung-resident eosinophils in BALB/c to B6 lung allografts with (blue) or without (red) CSB. Analysis of eosinophils from resting, untransplanted, B6 lungs shown as black line, while isotype control is shaded in gray. Representative of 3 to 5 separate transplants. (**C**) Histologic and flow cytometric analysis

of BALB/c→iPhil transplants depleted of eosinophils with treatment by DT or saline control. Representative histologic section (top) and ISHLT A grade of rejection (bottom). Scale bar: 100 μm. (**D**) Total number of graft-resident T cells (top left) and a representative plot of flow cytometrically analyzed lung digest defining $CD8^+$ T cells as $CD90^+CD8^+$ (top right). Total number of proliferating Ki-67^+ T cells (middle left) and a representative plot of Ki-67^+ $CD8^+$ T cells (middle right). Relative proportion of effector T cells (defined as $CD44^{hi}CD62L^{lo}$) (bottom left) and a representative plot of $CD8^+$ T cell effector differentiation (bottom right). All statistics performed by Mann-Whitney *U* test. $^*P < 0.05$; $^{**}P < 0.01$; $^{ns}P > 0.05$.

eosinophils with T lymphocytes. We thus cultured B6 T cells with BALB/c dendritic cells (DCs) in the presence of WT eosinophils, $iNOS^{-/-}$ eosinophils, or WT eosinophils separated from T cells by a semipermeable transwell, preventing direct T cell–eosinophil contact. Elimination of either eosinophil iNOS expression or eosinophil–T cell interaction ameliorated suppression of T cell responses (Figure 3B and Supplemental Figure 3B). We next extended these experiments by coculturing WT or $iNOS^{-/-}$ eosinophils with B6 T cells and BALB/c DCs, but removed eosinophils after 24 hours of culture. Even after this brief period of interaction, eosinophils still suppressed T cell proliferation (Figure 3C). Taken together, such data suggest that eosinophils suppress T cell responses through a contact- and iNOS-dependent mechanism early during the course of the immune response.

Eosinophils suppress T cell responses by altering the integrity of the TCR/CD3 complex. We next set out to determine how eosinophil-derived iNOS inhibits T cell activation. Previous work has described that iNOS-elaborated mediators such as nitric oxide (NO) and reactive oxygen species (ROS) can initiate T cell death (16), raising the possibility that eosinophils may control alloreactivity by altering T cell viability. However the presence of eosinophils in in vitro mixed leukocyte reactions (MLRs) did not decrease T cell viability and, surprisingly, even enhanced survival (Figure 4A). It has been described that iNOS-expressing, myeloid-derived suppressor cells may modify T cell reactivity in a contact-dependent fashion through posttranslational modification of key signaling intermediates within the IL-2 signaling pathway (17). IL-2–mediated T cell proliferation, however, was not affected upon culture with WT eosinophils (Supplemental Figure 4A).

Alternatively, modulation of TCR signaling has been described as another mechanism of iNOS-mediated immunoregulation. Specifically, it has been demonstrated that myeloid-derived suppressor cells can induce tumor-specific T cell tolerance by interfering with TCR signal transduction and altering the integrity of the TCR in a contact-dependent fashion (18, 19). We thus set out to evaluate signal transduction in $CD8^+$ T cells using a system of green fluorescent protein (GFP) driven by Nr4a1 (Nur77), an early TCR-responsive gene whose expression directly correlates with the strength of the TCR signal (20, 21). Indeed, we noted a near-complete ablation of TCR signal transduction in T cells cultured with WT, but not $iNOS^{-/-}$ eosinophils (Figure 4B and Supplemental Figure 4B). Further validation through transcriptome analysis of $CD8^+$ T cells from lung allografts depleted of eosinophils demonstrated a similar upregulation of Nr4a1 compared with $CD8^+$ T cells from eosinophil-sufficient allografts (Supplemental Figure 4C). To further explore this, we evaluated the structural integrity of the TCR from $CD8^+$ T cells cultured in the presence of WT or $iNOS^{-/-}$ eosinophils utilizing a technique of immunoprecipitation flow cytometry (IP-FCM) recently described by our group (19, 22). We noted that in the presence of WT but not $iNOS^{-/-}$ eosinophils the TCRβ subunit showed decreased association with both CD3ε and CD3ζ, suggesting dissociation of the TCR/CD3 complex. Taken together, our data suggest that eosinophils control T cell responses through contact- and iNOS-dependent inhibition of TCR stability and signal transduction.

Eosinophils mediate T cell suppression through PD-L1–mediated immunological synapse independent of professional APCs. Based on our finding that the suppressive capacity of eosinophils depends on their contact with T cells (Figure 3B), we next considered the possibility that professional APCs may act as a scaffolding to facilitate eosinophil–T cell contact. This assumption was based on our previous demonstration that T cells make stable and durable contact with lung-resident DCs (23) and the fact that eosinophils can mediate the recruitment and accumulation of DCs in asthma models (24, 25). To this end, we compared in a pairwise fashion the formation of eosinophil–T cell complexes in cocultures of B6 T cells stimulated with BALB/c bone marrow–derived DCs (BMDCs) or anti–CD3/CD28 agonistic antibodies. To our surprise, no increase in T cell–eosinophil interaction was evident in the presence of DCs. In fact, higher numbers of eosinophil–$CD8^+$ T cell complexes formed with CD3/CD28 stimulation (Figure 5A). A similar trend was evident for $CD4^+$ T cells, albeit at much lower levels of cell-to-cell contact (Figure 5A). In addition, the frequency of T cell–eosinophil interactions increased with the duration of cocultures for both $CD8^+$ and $CD4^+$ T cells (Figure 5B). Such data suggested that other factors, such as degree of T cell activation, may be responsible for contact formation.

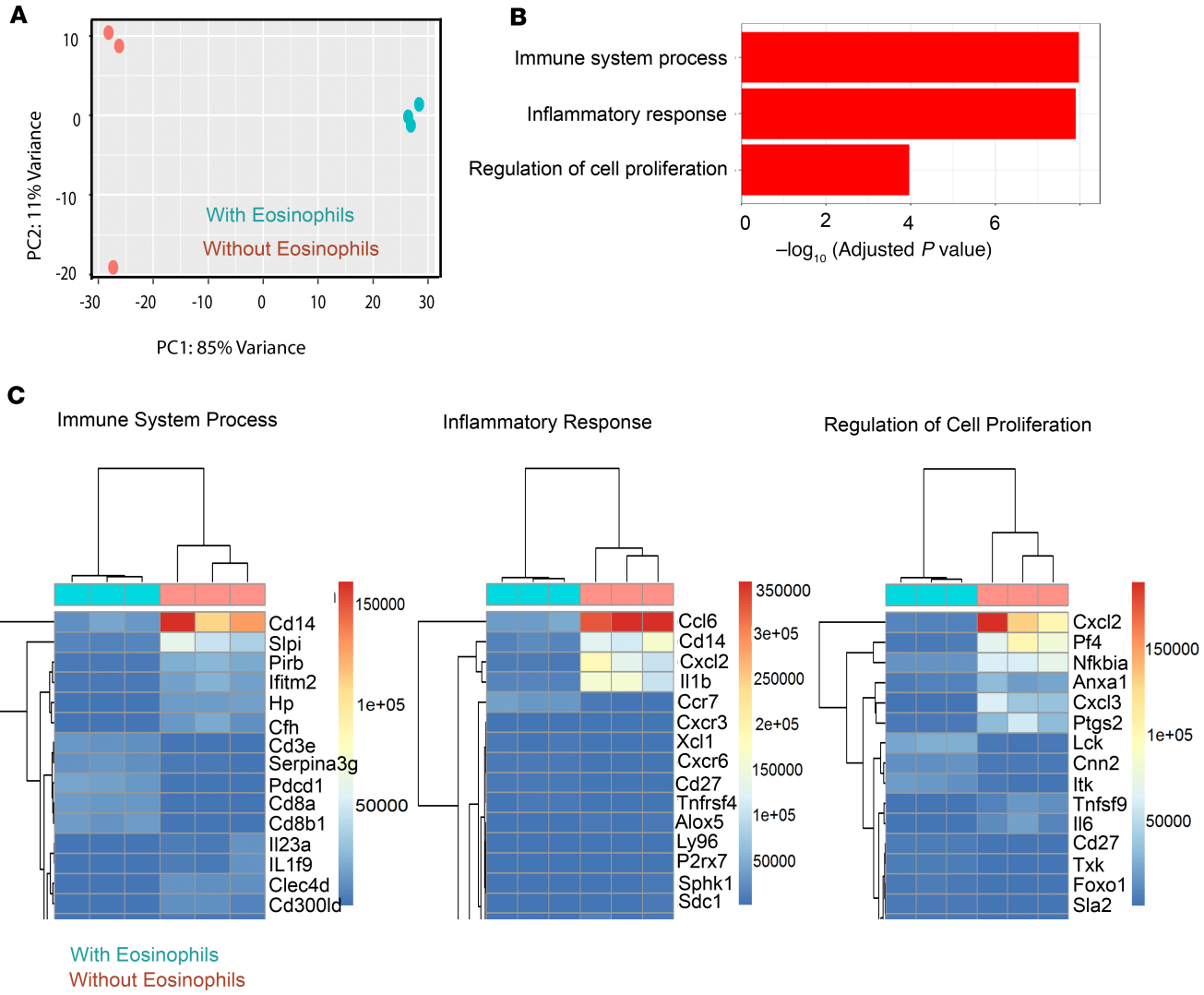


Figure 2. Gene expression analysis of lung allograft–resident CD8⁺ T cells in the presence or absence of eosinophils. (**A**) Graphic representation of the relationship among samples of the same group and the difference between the 2 groups of samples, based on the principle component analysis of the top 500 genes, selected by highest row variance. (**B**) Three of the top gene clusters upregulated in lung allograft–resident CD8⁺ T cells in eosinophil-deficient B6 recipients of BALB/c lungs as determined by gene ontology analysis using GeneSCF software. (**C**) Detailed heatmaps defining the relative levels of the top 15 genes in the inflammatory response, immune system process, and regulation of cell proliferation pathways defined as part of gene ontology analysis.

Based on these data, we next evaluated the role of surface junctional proteins in controlling T cell responses. E1 polarization of eosinophils specifically upregulated the expression of CD11b and PD-L1 (Figure 1B and Supplemental Figure 5A) but did not affect ICAM-1, -2, or LFA-1 levels (Supplemental Figure 5A). We thus initially focused on CD11b based on previous data implicating this integrin in mediating human granulocyte–T cell interactions (26). CD11b blockade, however, did not alter eosinophil–T cell contact (Supplemental Figure 5B). We then directed our attention to PD-L1 due to (a) its role in lung allograft tolerance and CD8⁺ T cell differentiation (27), (b) its upregulation during the course of E0 to E1 polarization (Supplemental Figure 5A), (c) the increase of its ligand PD-1 on lung-resident T cells after transplantation in vivo (Figure 5C) and in vitro during alloreactivity (Figure 5D), as well as (d) our previous data indicating that PD-L1/PD-1 interactions control T cell–DC synapse formation in the lung (27). Antibody blockage of PD-L1/PD-1 interactions led to a decrease in number of eosinophil–T cell complexes (Figure 5E) and increased T cell proliferation and effector differentiation (Figure 5F and Supplemental Figure 5C). Using ImageStream single-cell analysis of T cell and eosinophil cocultures, we noted that PD-L1 expression on eosinophils was highly polarized and predominantly sequestered to the membrane region in contact with T cells (Figure 5G).

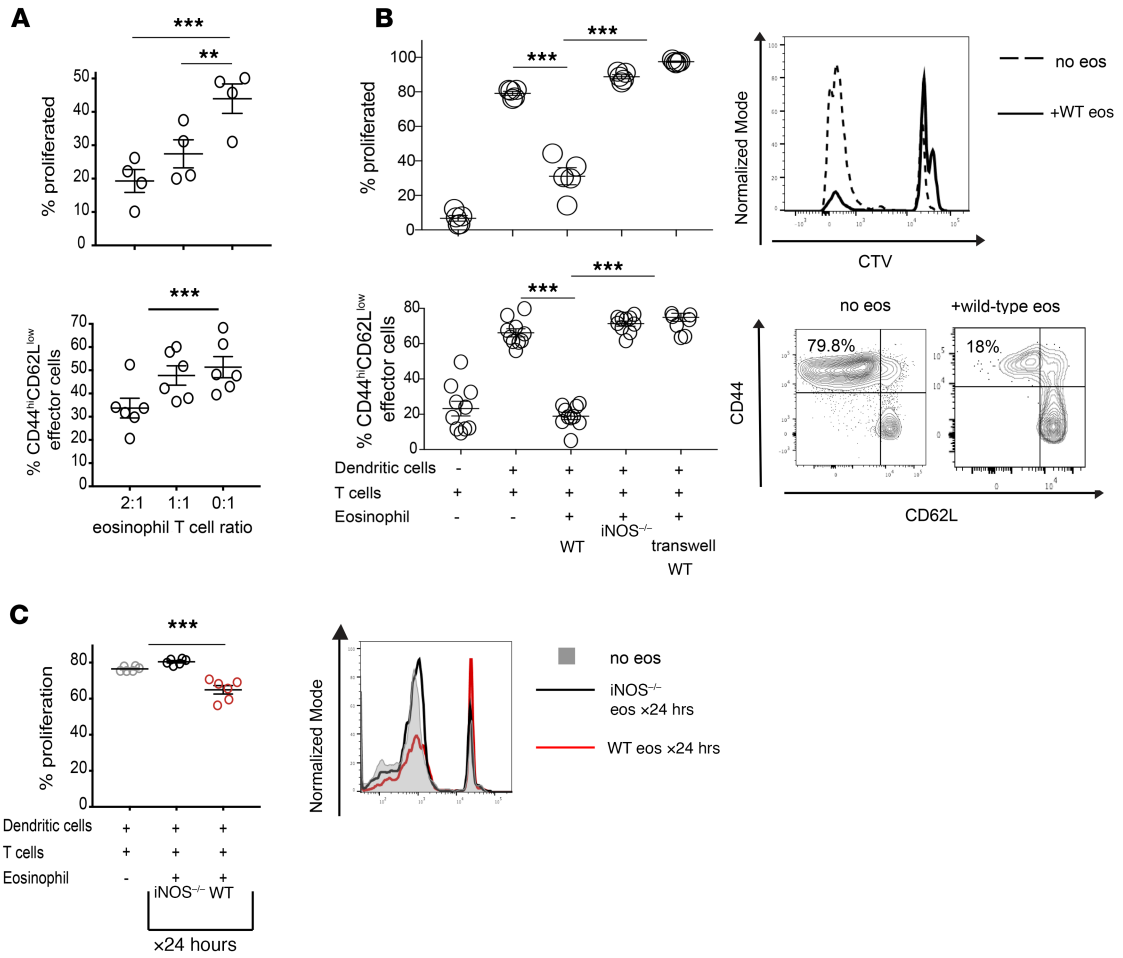


Figure 3. In vitro inhibition of T cells by E1-polarized eosinophils. (**A**) In vitro mixed leukocyte reactions (MLRs) established using anti-CD3/CD28 Dynabead stimulation of B6 T cells with varying ratios of E1-polarized B6 eosinophils added to the culture. The graph demonstrates percentage proliferation, as defined by the dilution of the CellTrace Violet (CTV) proliferation dye, and effector differentiation, as defined by the percentage of $CD44^{hi}CD62L^{lo}$ $CD8^+$ T cells after 5 days of coculture. Representative data from 1 out of 3 similar experiments. (**B**) Proliferation and effector differentiation of B6 $CD8^+$ T cells stimulated by BALB/c dendritic cells in a coculture with a 2:1 ratio of eosinophils to T cells. For some conditions, WT or $iNOS^{-/-}$ eosinophils were added directly to the dendritic cell–T cell cocultures, while in other conditions the eosinophils were separated from the dendritic cell–T cell cocultures by a semipermeable membrane. Summary of data shown on the left, and representative flow cytometry plots on the right. Representative data from 1 out of 3 similar experiments. (**C**) MLRs, similar to those demonstrated in **A** were set up with a 2:1 ratio of eosinophils to T cells, except E1-polarized eosinophils were removed from the culture after 24 hours (X24 hrs) and T cell proliferation was analyzed on day 5 of the MLR. Summary of data shown on the left, and representative flow cytometry plot on the right. All statistics performed by Mann-Whitney *U* test. $^{**}P < 0.01$; $^{***}P < 0.001$.

Thus, eosinophils made direct contact with T cells through PD-L1, which was critical for their suppressive effect. Of note, $CD8^+$ T cells expressed higher levels of the PD-L1 receptor PD-1 compared with $CD4^+$ T cells (Figure 5, C and D). Such data provide a possible explanation of why eosinophil-mediated interaction and suppression was more pronounced for $CD8^+$ rather than $CD4^+$ T cells. Interestingly, PD-L1 levels were similar between WT and $iNOS^{-/-}$ eosinophils (Supplemental Figure 5A), despite the fact that $iNOS^{-/-}$ eosinophils were unable to inhibit T cell proliferation (Figure 3B). It is thus unlikely that eosinophil-derived PD-L1 directly contributes to downregulation of T cell responses through engagement and signaling via PD-1, but rather acts only indirectly by mediating cell to cell interaction.

Eosinophils do not directly inhibit allogeneic professional APCs. In addition to their direct effect on T cell activity, the possibility existed that eosinophils may also influence T cell responses by altering the antigen-presenting capacity of professional APCs. This notion is based on work by us as well as others that suggests that E2-polarized eosinophils could modulate APCs to affect Th2 pulmonary immune responses (14, 24, 28). However, in our in vitro MLRs we detected only limited numbers of DC-eosinophil interactions, similar to the low number of $CD4^+$ T cell–eosinophil interactions described above (Figure 6A).

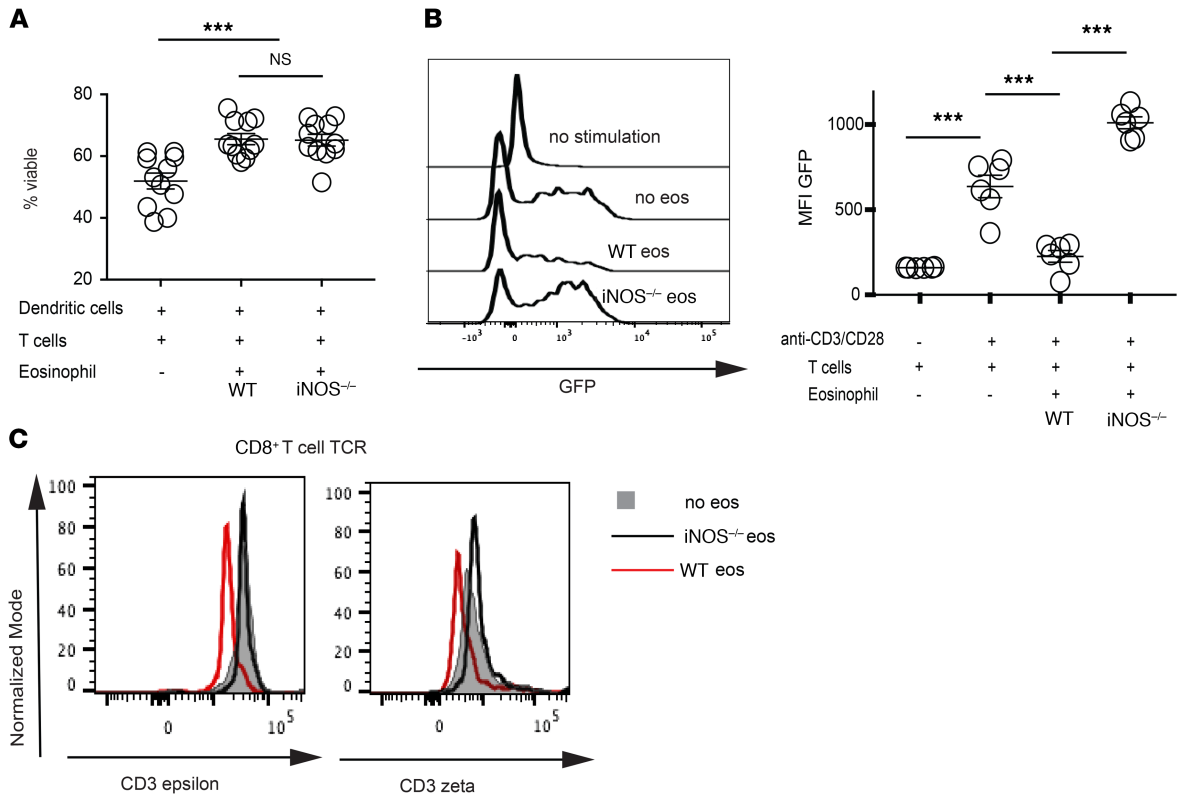


Figure 4. Eosinophils alter TCR signal transduction. (**A**) In vitro MLRs established using the coculture of bone marrow–derived BALB/c dendritic cells, and B6 T cells with a 2:1 ratio of E1-polarized B6 eosinophils directly added to the culture. T cell viability was determined flow cytometrically after 5 days of coculture with no, WT, or iNOS$^{-/-}$ eosinophils as described in the graph. Representative data from 1 out of 3 similar experiments. (**B**) In vitro MLRs established using the coculture of anti–CD3/CD28 Dynabeads with Nur77 T cells and a 2:1 ratio of E1-polarized eosinophils. Nur77-driven GFP expression was used as a gauge of TCR stimulation in CD8$^+$ T cells after 36 hours of coculture with no, WT, or iNOS$^{-/-}$ eosinophils. Representative of 1 out of 3 separate experiments. (**C**) Evaluation of the TCR/CD3 complex integrity by quantification of TCRβ immunoprecipitations with coassociated CD3ζ or CD3ε on CD8$^+$ T cells isolated from in vitro MLRs in the presence of no eosinophils (gray) versus WT (red line) or iNOS$^{-/-}$ eosinophils (black line). Data representative of 1 out of 5 mice. All statistics performed by Mann-Whitney *U* test. ***$P < 0.001$, $^{ns}P > 0.05$.

In addition, eosinophils did not alter the maturation of bone marrow–derived myeloid cells in vitro (Supplemental Figure 6A). To further evaluate the role of eosinophils in controlling myeloid cell activation in vivo, we next transplanted BALB/c lungs to either DT-treated or control B6 iPHIL mice. Both CD11c$^+$CD64$^+$ interstitial macrophages, as well as CD11c$^+$CD103$^+$CD64$^-$ dendritic cells, expressed higher levels of MHC I and MHC II and costimulatory markers following eosinophil depletion (Figure 6B). Such differences in APC maturation, however, were absent in T cell–depleted mice (Figure 6C), suggesting that effects of T cell activation, rather than the direct action of eosinophils, were responsible for the activation of myeloid cells. Taken together with the T cell–eosinophil contact data, these results show that eosinophil-dependent immunoregulation is primarily due to their direct interactions with T cells and not myeloid cells.

Augmenting eosinophil recruitment to the lung downregulates alloimmunity and acute graft rejection. To evaluate whether eosinophils could be used as a cellular therapy to downregulate alloimmune responses after pulmonary transplantation, we injected 15 × 10^6 B6 eosinophils into B6$^{CD45.1+}$ congenic recipients of BALB/c lungs at the time of engraftment. We noted that only limited numbers of injected eosinophils homed to the lung graft, with severe graft rejection and CD8$^+$ T cell effector differentiation despite adoptive transfer (Supplemental Figure 7A). Thus, an alternative approach was needed to evaluate the role of augmented eosinophil migration on alloimmune responses. The chemokines eotaxin 1 (CCL11) and eotaxin 2 (CCL24) promote eosinophil migration and homing (29), while IL-5 promotes eosinophil survival (30). We thus administered a combination of eotaxin 1, 2, and IL-5 intratracheally (31) to B6 recipients of BALB/c allografts immediately after as well as 24 hours following

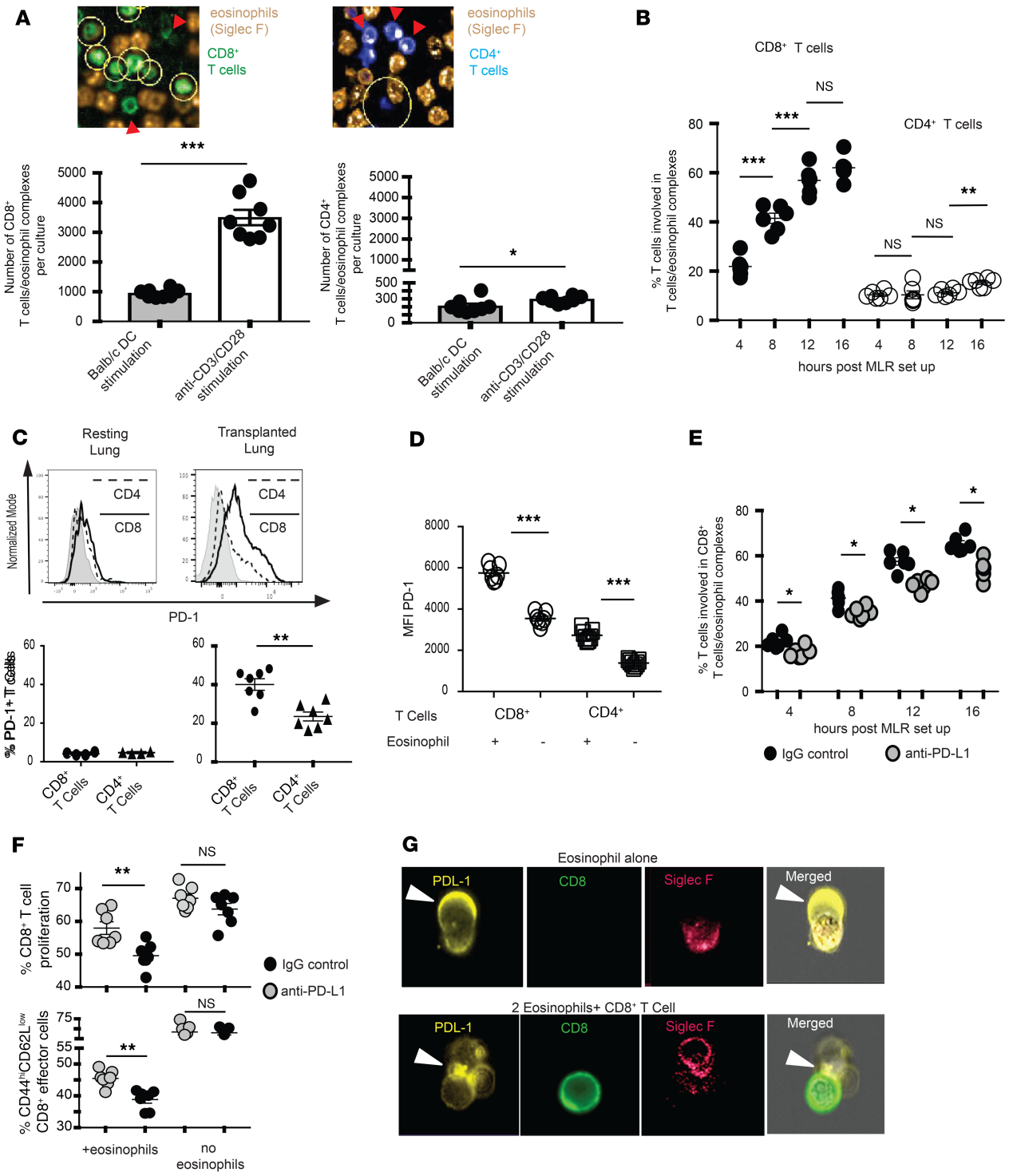


Figure 5. PD-L1–mediated T cell–eosinophil interaction. (**A**) In vitro MLRs established using the coculture of bone marrow–derived BALB/c dendritic cells or anti–CD3/CD28 Dynabeads, and fluorescently labeled CD8⁺ and CD4⁺ B6 T cells with a 2:1 ratio of E1-polarized fluorescently labeled B6 eosinophils. Eosinophil–T cell interactions were analyzed using Harmony Software. Yellow circles in the top graphic representation demonstrate Harmony Software–detected T cell–eosinophil interactions, which are quantitated in graphic form at the bottom. (**B**) Quantification of T cell–eosinophil interaction during 16 hours of coculture in vitro as determined by Harmony Software analysis of live confocal microscopy. (**C**) PD-1 expression in CD4⁺ and CD8⁺ T cells of resting and transplanted murine lungs in vivo. Graphic representation at the top, and quantification of percentage of T cells expressing PD-1 at the bottom. (**D**) PD-1 expression on T cells in in vitro MLRs stimulated with anti–CD3/CD28 Dynabeads in the presence or absence of WT eosinophils. (**E**) CD8⁺ T cell–eosinophil interactions in the presence of PD-L1 blockade during 16 hours of coculture in vitro, as determined by Harmony Software analysis of live confocal microscopy. (**F**) CD8⁺ T cell proliferation and effector differentiation in the presence or absence of eosinophils and PD-L1 blockade in in vitro MLRs with anti–CD3/CD28 Dynabead stimulation. All MLRs in **A**–**F** demonstrate 1 experiment from 2 to 3. (**G**) ImageStream analysis of eosinophil–T cell MLRs for surface analysis of PD-L1 expression and polarization. All statistics performed by Mann-Whitney *U* test. $^{*}P < 0.05$; $^{**}P < 0.01$; $^{***}P < 0.001$; $^{ns}P > 0.05$.

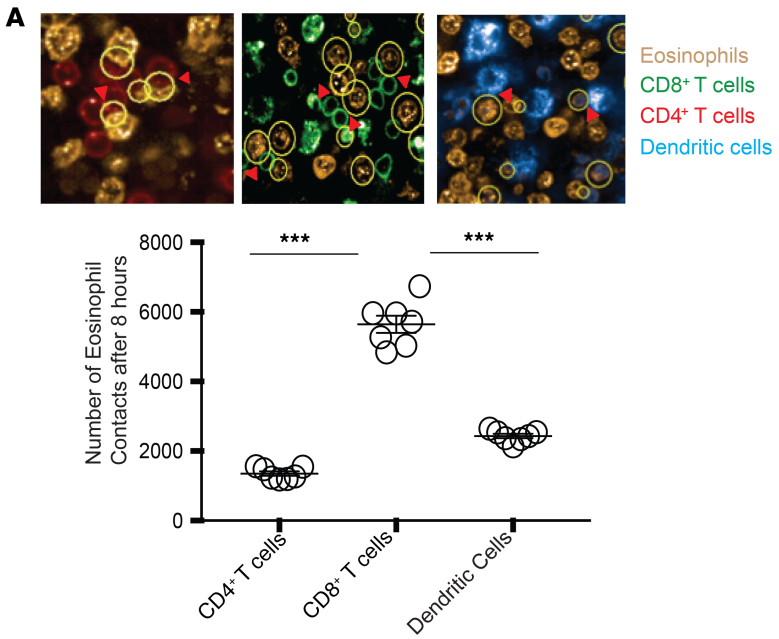
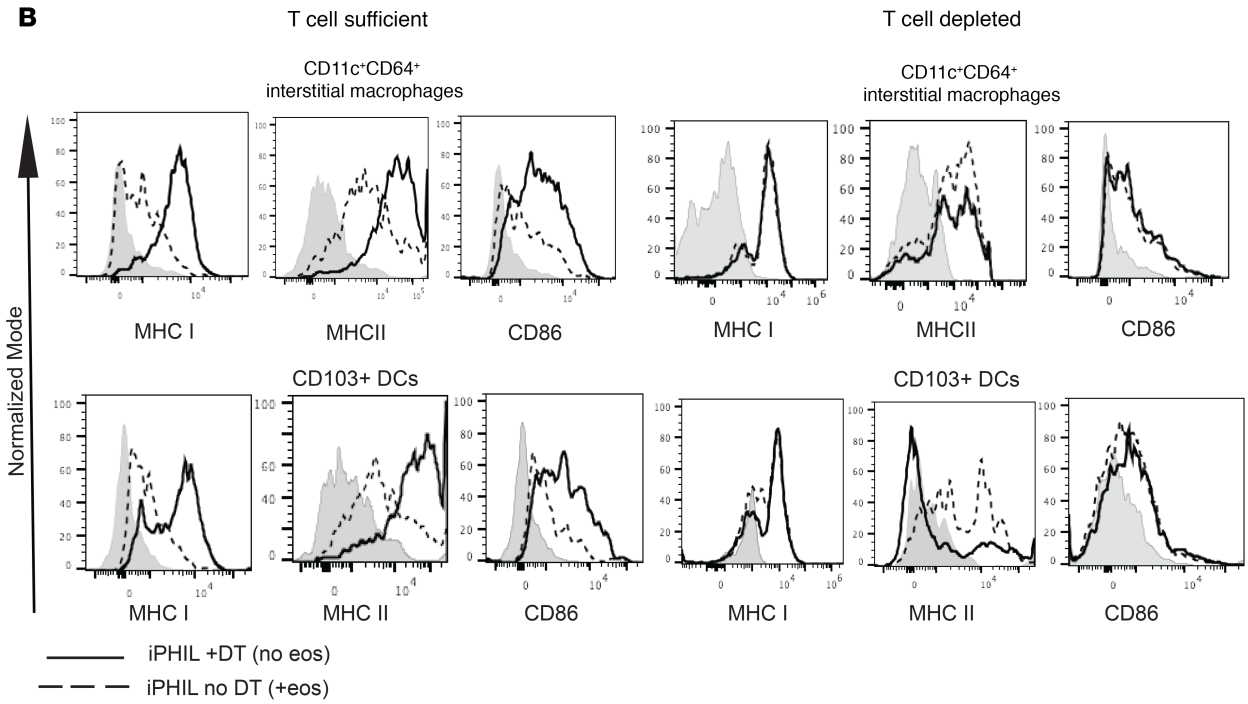


Figure 6. Eosinophil interaction with and phenotypic alteration of myeloid cells. (**A**) In vitro MLRs established using the coculture of fluorescently labeled bone marrow–derived BALB/c dendritic cells, and fluorescently labeled $CD8^+$ and $CD4^+$ B6 T cells with a 2:1 ratio of E1-polarized fluorescently labeled B6 eosinophils. Eosinophil–T cell–dendritic cell interactions were analyzed using Harmony Software, with the yellow circles in the top graphic representing interactions. The bottom panel represents the number of eosinophil contacts with $CD4^+$ T cells, $CD8^+$ T cells, or dendritic cells. Data representative of 2 separate experiments. (**B**) BALB/c lungs were engrafted into B6 iPHIL mice treated with DT (eosinophil deficient) or saline (eosinophil sufficient). The phenotypes of $CD11c^+CD64^+$ interstitial macrophages and $CD103^+$ dendritic cells were evaluated flow cytometrically in engrafted lungs in the presence of the full complement of T lymphocytes (left panels) or after depletion of both $CD4^+$ and $CD8^+$ T cells (right panel). Representative of 2 separate sets of transplants. All statistics performed by Mann-Whitney *U* test. $^{***}P < 0.001$.



lung transplantation, and evaluated the immune response 7 days later in the absence of conventional immunosuppression or CSB. Compared with saline controls, eotaxin-treated mice manifested less inflammation and decreased grade of rejection using the International Society for Heart and Lung Transplantation (ISHLT) A Grade criteria (Figure 7A). Eotaxin and IL-5 administration resulted in higher numbers of graft-resident eosinophils (Figure 7B). Although the total number of $CD8^+$ T cells in the lung graft did not change, there were significantly fewer $CD8^+CD44^{hi}CD62L^{lo}$ effector cells in eotaxin/IL-5–treated lungs (Figure 7C and Supplemental Figure 7B). Eotaxin/IL-5–mediated immunosuppression was not evident in eosinophil-depleted mice (Supplemental Figure 7C), indicating that this regimen was not directly immunosuppressive on T cells, but relied on eosinophil migration for its function. Collectively, our data suggest that augmenting eosinophil accumulation can be utilized to downregulate lung alloimmune responses.

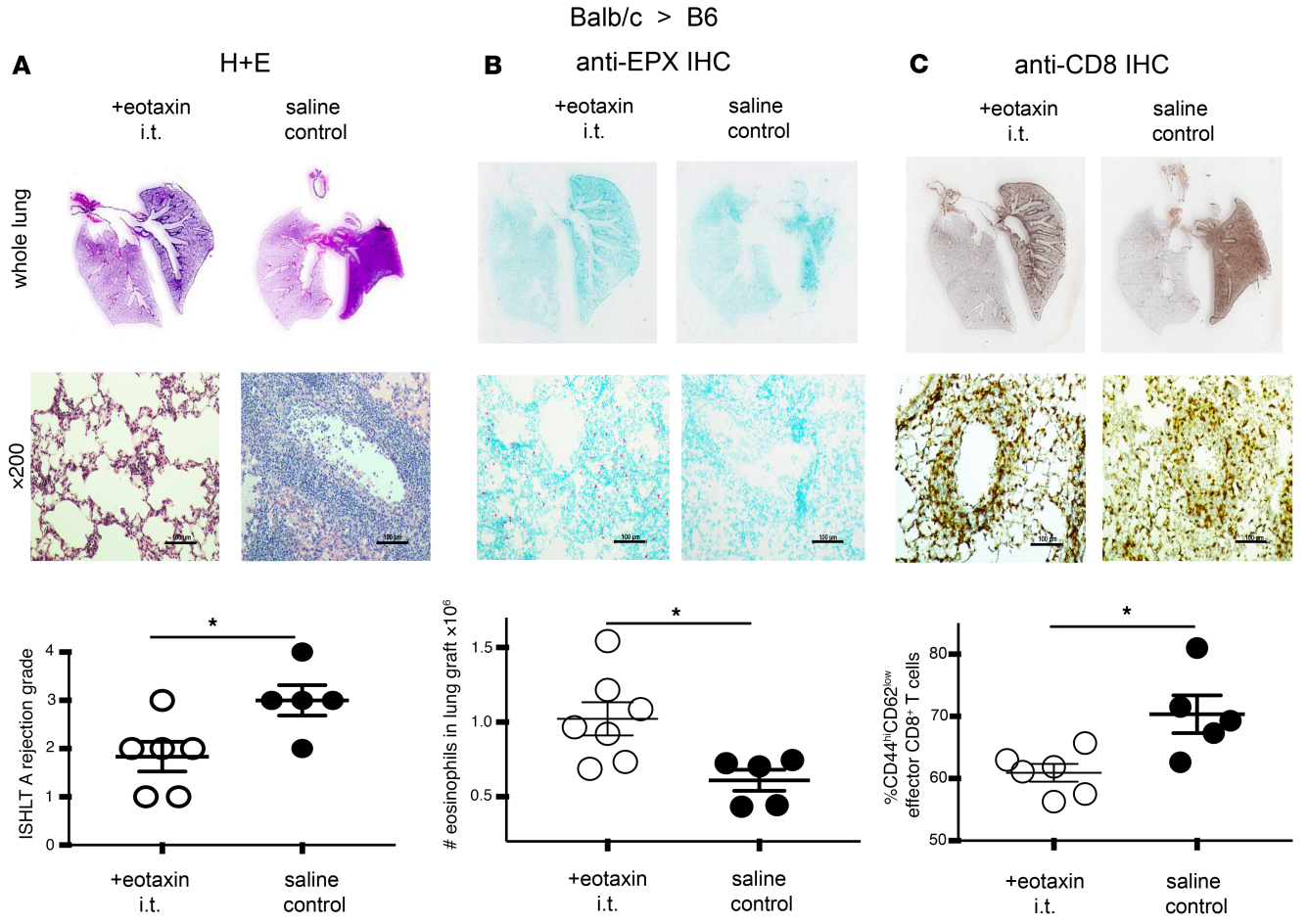


Figure 7. Rejection of BALB/c→B6 lung grafts treated with intratracheal eotaxin 1, 2, and IL-5. BALB/c lungs were transplanted into B6 recipients, which were treated with an intratracheal chemokine and cytokine cocktail of eotaxin 1, 2, and IL-5 immediately after engraftment and 1 day after transplantation. Lung grafts were evaluated flow cytometrically and histologically after 7 days for rejection (**A**), total eosinophil content (**B**), and $CD8^+$ T cell differentiation (**C**). Histologic analysis for ISHLT grade of rejection was performed on slides stained with hematoxylin and eosin (H&E), and eosinophil peroxidase immunohistochemistry was performed to evaluate eosinophil orientation in the tissue (eosinophils stained red). Scale bars: 100 μm. All statistics performed by Mann-Whitney *U* test. $^*P < 0.05$.

Discussion

Unlike other solid organ allografts, lungs are unique, as they are continuously exposed to the external environment as part of their natural function of gas exchange. For these reasons, unique pulmonary-specific immunoregulatory pathways have developed to eliminate environmental pathogens while resolving benign nonpathogenic insults. Pathways for rapid downregulation of inflammatory responses have also evolved out of necessity to ameliorate undue damage to bystander pulmonary parenchyma during the course of the immune response. Eosinophils are bone marrow–derived granulocytes that are known for their ability to combat infection and are found in low levels at baseline in healthy lungs (14). Both experimental and clinical eosinophil deficiency renders hosts more susceptible to infectious disease, especially by fungal and parasitic organisms (32, 33). Consistent with these IL-4–dominated parasitic Th2 responses, eosinophils have also been well described to contribute to the initiation, propagation, and possibly resolution of allergic environmental asthma (34). While the role of eosinophils in other immunologic processes is still under investigation, here we identify that in the setting of lung transplantation, eosinophils may function similarly to granulocytic myeloid-derived suppressor cells by downregulating T cell immune responses through the modification of TCR/CD3 stability and signal transduction (18, 19).

Current clinical status of solid organ transplantation involves the use of global immunodepleting or immunosuppressive drugs. Standard protocols for surveillance have been designed to diagnose inflammatory changes through routinely scheduled biopsies of grafts (1). Any increase in inflammation is treated through upregulation of immunosuppression to combat what is considered early rejection (1).

For these reasons, eosinophil-related inflammatory changes and organ infiltration have been proposed as both a mediator and diagnostic feature of liver allograft rejection (35). In direct contrast to this notion, we have demonstrated that proinflammatory feedback loops, of which eosinophils are a critical component, play a critical role in tolerance induction in the lung (7). Disruption of such loops, through depletion of either $CD8^+$ T cells or eosinophils, prevents CSB-mediated graft acceptance (5, 7). Here we extend those findings to describe that eosinophils contribute to the downregulation of lung allograft rejection even in the absence of immunosuppression. Our data thus solidify the role of eosinophils as an exclusive and, we believe, previously unrecognized regulatory leukocyte in the lung. Based on these data, as well as on select human observational studies, it is possible that eosinophils may play a similar immunosuppressive role in other organ transplants (36). Furthermore, recent data from the University of Zurich by Arnold and colleagues demonstrate that eosinophils may interfere with Th1-mediated clearance of gastrointestinal pathogens (37). It is thus possible that the eosinophils may downregulate immune responses across multiple disease processes.

We also demonstrate in our system that eosinophils interfere with TCR stability and signal transduction as their mechanism of immunosuppression. In this manner, eosinophil-mediated immunoregulation in the lung allograft mirrors that of malignancy-related immunosuppression, where multiple mechanisms function to downregulate TCR signaling and mediate tumor escape (18, 19). This finding also creates an appealing aspect for tolerance induction, as eosinophils can effectively alter the "priming" phase of alloreactivity that occurs immediately after engraftment. Since eosinophils accumulate in the allograft early after engraftment (7), they affect allorecognition at early time points and may alter the frequency of alloreactive T cell clones for the life of the graft. By interfering with the strength of TCR signal transduction, eosinophil-mediated downregulation of immune responses may mirror CSB shaping of the T cell repertoire toward lower-affinity clones (38). It is thus possible that such early action may indirectly affect long-term immunologic graft survival. Whether eosinophils are critical or dispensable at later time points in the lung has yet to be resolved.

Despite the ever-growing appreciation of inhibitory ligand-receptor interactions in cancer (39), the biological role of PD-L1 in transplant tolerance is just now being appreciated. Our data thus support the early reports by Tanaka and colleagues demonstrating that PD-L1 expression plays a role in tolerance induction of cardiac allografts (40). A recent report from our group that PD-1 blockade can break lung allograft tolerance supports this notion as well (27). Interestingly, we now describe that PD-1/PD-L1 interactions increase the number of T cell–eosinophil contacts (Figure 5E). This is in direct contrast to the case for $CD11c^+$ DCs, where PD-L1/PD-1 interactions actually decreased T cell dwell time (27). Taken together, our results suggest that T cell PD-1 expression plays a dual role in facilitating lung allograft tolerance by both decreasing interaction with prorejection APCs such as $CD11c^+$ DCs, while at the same time augmenting contact with regulatory cells such as eosinophils. Since $iNOS^{-/-}$ eosinophils still express PD-L1 upon E0 to E1 polarization (Supplemental Figure 5A), we can assume that, at least in our model, eosinophil expression of PD-L1 contributes to cell-cell interactions and not to direct inhibition of T cell activation through PD-1 engagement. This finding sets PD-L1–dependent allograft tolerance apart from some models of tumor-related immunosuppression, where direct signaling through PD-1 leads to downregulation of the T cell responses (41). However, our data support other models where PD-L1 expression correlates with, but does not directly contribute to, the downregulation of T cell function through PD-1 engagement (42). Thus, our data extend the notion that the role of PD-L1 in immune suppression must be APC and context dependent.

While PD-L1/PD-1 seems to control cell contact, our data further support the dominant and near-exclusive role of iNOS in eosinophil-mediated downregulation of immune responses. The observation that both contact and iNOS expression determines eosinophil-specific inhibition of T cell proliferation (Figure 3B) further strengthens the notion that environmental polarization of eosinophils is critical for their suppressive function. It is important to point out that in the absence of exogenous Th1-polarizing cytokines, such as IFN-γ and TNF-α, neither PD-L1 nor iNOS is expressed in E0 unpolarized resting eosinophils (Figure 1, A and B, and Supplemental Figure 5A). Only upon polarization to the E1 phenotype do such suppressive mediators become evident (Supplemental Figure 5A). IL-4– and IL-33–polarized E2 eosinophils also do not express iNOS (Figure 1, A and B), furthering the notion that the environmental context controls eosinophil-mediated immunoregulation in our system.

Unlike the case for most other organs, where access for local drug delivery can be problematic, intratracheal administration of biological mediators can readily be utilized to alter the course of pulmonary immune responses (43, 44). Based on this notion, we now demonstrate that local administration of eosinophil-specific

chemokines and cytokines can alter lung allograft rejection in an eosinophil-dependent fashion. Such data open the possibility of accentuating naturally occurring tolerogenic feedback loops in order to downregulate lung graft rejection in the absence of global nonspecific immunosuppression.

Methods

Animals

C57BL/6$^{CD45.2+}$ (B6) (H2^{b}), B6.SJL/BoyJ(B6$^{CD45.1+}$) (H2^{b}), BALB/c (H2^{d}), and Nur-77 GFP (C57BL/6-Tg(Nr4a1EGFP/cre)820Khog/J) mice were obtained from The Jackson Laboratory. iPHIL mice (expressing the DT receptor under the control of an eosinophil peroxidase–specific promoter) and hypereosinophilic IL-5–transgenic mice (NJ.1638) were developed in our laboratory at the Mayo Clinic (15, 45), and bred and maintained at the vivarium facility at the University of Virginia School of Medicine. For in vitro experiments, iNOS$^{-/-}$ hypereosinophilic mice were generated by crossing the NJ1638 strain with the B6.129P2-*Nos2*^{tm1Lau}/J (iNOS$^{-/-}$) strain (Jackson Laboratory) for at least 3 generations. Such mice were then maintained as a colony by crossing the NJ1638 iNOS$^{-/-}$ strain with WT iNOS$^{-/-}$ mice. The animals passed all necessary genotyping screening or quarantine serological tests (for those that were transported from one university to the other) before they were used in this study. Mice used as donors were 5- to 8-week-old males; those used as graft recipients in this study were also males at 2 to 4 months of age, while both male and female hypereosinophilic mice were used when they were 3 to 7 months old for eosinophil isolation.

Surgery and transplantation

Orthotopic transplantation of a left lung allograft was carried out according to our previous reports (46, 47). To achieve allograft acceptance, mice were treated with double costimulatory blockade of the CD28/B7 and the CD40/CD40L pathways as previously described (48).

Histology

Lungs were fixed in formalin, sectioned, and stained with hematoxylin and eosin (H&E). A lung pathologist blinded to the experimental conditions graded graft rejection using standard criteria (ISHLT A Grade, developed by the Lung Rejection Study Group (49).

Immunohistochemistry

Formalin-fixed lung tissues embedded in paraffin were sectioned, subjected to antigen retrieval, and stained with either mouse anti–mouse eosinophil peroxidase and secondary goat anti-mouse antibodies or rat anti–mouse CD8 and secondary donkey anti-rat antibodies for the detection of eosinophils or CD8^{+} cells, respectively, as previously reported (50, 51). The protocol for eosinophil detection included blocking with Dual Endogenous Blocking Solution (Dako) and donkey serum before incubation in the primary antibody, while horse serum was used for the initial blocking of the tissue slide for CD8 staining and detection.

Flow cytometry

For flow cytometric analysis, lung tissue derived from resting or graft recipient mice was well minced with scissors and digested by placing it into RPMI 1640 medium (Thermo Fisher Scientific) containing 0.5 mg/ml collagenase II (Worthington Biochemical Corporation) and 5 U/ml DNAse (Sigma-Aldrich) for 60 minutes at 37°C in a shaker. The digested lung tissue was passed through a 70-μm cell strainer and treated with ACK lysing buffer (Lonza) to remove red cell contamination. This digestion method has been previously described (7).

Measuring the subunit ratios within the TCR/CD3 complex via IP-FCM was performed as previously described (19). Briefly, CD8^{+} T cells were purified from a 36-hour culture where T cells were activated by plate-bound CD3/CD28 in the presence of no eosinophils, WT eosinophils, or iNOS$^{-/-}$ eosinophils. For evaluation of the TCR complex, the CD8^{+} T cells were lysed in 1% digitonin isotonic lysis buffer, and postnuclear lysates were incubated for IP with a monoclonal antibody specific for TCRβ (clone H57-597) to immunoprecipitate the native TCR/CD3 complexes. With the β chain functioning to pull down the TCR, such captured complexes were then probed in parallel with PE-conjugated monoclonal antibodies specific for CD3ζ (clone 6B10) or CD3ε (clone 2C11) for evaluation of TCR complex integrity.

All antibodies for flow cytometry were primarily fluorochrome-conjugated anti-mouse monoclonal antibodies, mostly derived from rat. Thus, staining of samples was by direct immunofluorescence.

Intracellular staining was performed as previously described (7). The following antibodies were purchased from BD Biosciences: anti-iNOS FITC (clone 6/iNOS/NOS type II), anti–PD-L1 PE or brilliant violet (BV)-421 (clone MIH5), and anti–Siglec-F PE or PerCPCy5.5 (clone E50-2440). Antibodies purchased from Biolegend include anti-CD68 Alexa-488 or BV-421 (clone FA-11); anti-CD206 FITC, APC, or BV-421 (clone C068C5); anti-CD64 PE-Cy7 (clone X54-5/7.1); and anti-CCR3 PE or PE-Cy7 (clone J073E5). The following antibodies were purchased from Thermo Fisher Scientific–eBiosciences: anti-CD45 eFluor-450 or eFluor-506 (clone 30-F11); anti-CD45.2 eFluor-450 or eFluor-506 (clone 104); anti-CD45.1 APC-eFluor-780 or eFluor 506 (clone A20); anti-CD11b FITC or APC-eFluor-780 (clone M1/70); anti-CD86 PE or PE-Cy7 (clone GL1); anti-CD80 APC or PE-Cy7 (clone 16-10A1); anti–MHC-II (IA/IE) APC-eFluor-780 (clone M5/114.15.2); anti-CD8a FITC, PerCPCy5.5, or APC-eFluor-780 (clone 53-6.7); anti-CD90.2 FITC or APC-eFluor-780 (clone Thy-1.2); anti-MHC-I ($H2K^b$) PE or APC (clone AF6-88.5.5.3); anti-MHC-I ($H2K^d$) PerCP-eFluor710 (clone SF1-1.1.1); anti–MHC-II (IA/IE) Alexa-488 (clone M5/114.15.2); anti–MHC-II (IA-b) PE (clone AF6-120.1); anti–MHC-II (IA-d) APC (clone AMS-32.1); anti-CD11c PerCPCy5.5 or eFluor-506 (clone N418); anti-F4/80 FITC or PE (clone BM8); CD103 eFluor 450 (clone 2E7); anti–PD-1 APC (clone J43); anti-CD40 APC (clone 1C10); anti-CD4 APC or eFluor 405 (clone RM4-5); anti-CD44 PE or PerCPCy5.5 (clone IM7); anti-CD62L PE-Cy7 (clone MEL-14); anti-CD101 PE (clone Moushi101); and anti–Ki-67 PE (clone SolA15). All fluorochrome-conjugated antibodies were matched with the corresponding IgG isotypes as antibody controls. In addition, fluorescence-minus-one (FMO) controls were also used to separate the negative and positive populations. Dead cells were excluded with Live/Dead Fixable Stain (Thermo Fisher Scientific). To block nonspecific binding to Fc receptors, we used anti–CD16/CD32 (Thermo Fisher Scientific) (clone 93). Cells expressing various markers of interest were acquired in a BD FACSCanto II, equipped with 3 lasers for 10-parameter detection (BD Biosciences). Quality controls were performed daily on the flow cytometers according to the manufacturer's instructions. Analysis of flow cytometry data was done with FlowJo software, version 10.

Image cytometry

ImageStream Mark II (MilliporeSigma) was used to visualize and study immune synapse formation between eosinophils and T cells. The procedure is as previously reported (52), with slight modifications. Briefly, a combination of purified T cells (stimulated with DCs or anti–CD3/CD28 agonistic antibodies) and eosinophils were incubated for 24 hours to establish contacts. Cells were washed in 2% FBS in PBS and centrifuged at 200 *g* for 4 minutes. Cells were fixed with BD Cytofix (Fixative Buffer) for 20 minutes and washed with BD Perm/Wash buffer at 200 *g* for 4 minutes. Cells were stained with a combination of rat anti-mouse antibodies, including anti-CD8 FITC (clone 53-6.7), anti–PD-L1 PE (clone MIH5), and anti–Siglec-F PerCpCy5.5 (clone E50-2440), and incubated for 30 minutes at 4°C. The cells were washed in BD Perm/Wash buffer at 200 *g* for 4 minutes and resuspended in 2% FBS in PBS for acquisition. The image data were visualized and analyzed with the Ideas Software version 6.

Fluorescence-activated cell sorting for lung eosinophils

Eosinophils were sorted as $CD45^+CD11b^+Siglec\text{-}F^+CD11c^-$ cells following the staining of digested lungs with a panel of fluorochrome-conjugated antibodies similar to the ones used for flow cytometry. Sorting was done using the BD Influx (BD Biosciences).

Isolation, culture, and polarization of mouse peripheral blood eosinophils

Eosinophils were isolated from peripheral blood of NJ.1638 or NJ1638 $iNOS^{-/-}$ strain after density-dependent separation of the eosinophil-rich white blood cells using a combination of Histopaque 1119 and 1083 (Sigma-Aldrich) at a ratio of 1:9, followed by negative selection of a greater than 98% pure eosinophil population after incubation of white blood cells with a combination of CD45R/B220 and CD90.2/Thy-1.2 immunomagnetic beads (Miltenyi Biotec). The purity of eosinophils was confirmed by flow cytometry ($CD45^+CD11b^+Siglec\text{-}F^+CD11c^-$ cells). The details of the cell preparation and eosinophil purification protocol are as we have previously described (9). For in vitro experiments, purified eosinophils were cultured at 5×10^5/ml for 18 to 24 hours in RMPI-1640 media (containing glutamine and 25 mM HEPES) (Thermo Fisher Scientific) supplemented with 10% FBS, 10 U/ml penicillin, 10 μg/ml streptomycin, 29.2 μg/ml L-glutamine, and 55 μM β-mercaptoethanol. Eosinophils maintained in an unpolarized (E0) state were cultured with 10 ng/ml IL-5. Th1-polarized eosinophils (E1) were cultured with 10 ng/ml IL-5, 15 ng/ml IFN-γ, and 15 ng/ml TNF-α, while Th2-polarized eosinophils (E2) were cultured with 10 ng/ml IL-5,

30 ng/ml IL-33, 10 ng/ml IL-4, and 10 ng/ml GM-CSF. All cytokines and growth factors used for eosinophil polarization culture were recombinant proteins purchased from Peprotech.

In vitro MLR

BMDCs (53) from BALB/cJ mice or anti–CD3/CD28 agonistic antibodies (Dynabeads or plate bound, Thermo Fisher Scientific) were used to stimulate Thy1.2-positive (CD90.2-positive) cells from B6, B6.SJL/BoyJ, or Nur77^{GFP} mouse splenocytes. After careful titration, the volume of Dynabeads used was 5.0 μl for 1 ml of media containing 1 × 10^6 T cells. Such concentration resulted in 50% to 90% T cell proliferation after 5 days of culture. To prepare the coated plate used for a maximum of 48 hours of culture, the concentration of soluble anti–CD3/CD28 agonistic antibodies used were 2.0 μg/ml anti-CD3 and 1.0 μg/ml anti-CD28 agonistic antibodies in PBS. A small volume (250 μl) of the solution was used to coat 1 well of a 96-well round-bottom plate. The CD90.2$^+$ cells were obtained by positive selection with magnetic-activated cell separation (MACS) using Mouse CD90.2 MicroBeads (Miltenyi Biotec). In some experiments, where we needed to reisolate CD8$^+$ T cells from the MLRs after culture, T cells were isolated from the splenocytes by negative selection using Mouse Pan T Cell Isolation Kit II (Miltenyi Biotec). CD90.2$^+$ cells or purified T cells were cultured together with the BMDCs in a round-bottom 96-well plate at a ratio of 10:1 (T cells/BMDCs). In some experiments, eosinophils isolated from NJ1638 or NJ1638 iNOS$^{-/-}$ mice were also added to the culture at 2:1 eosinophil/T cell ratio or as stated in the results section. Cells were cultured at 37°C with addition of 5% carbon dioxide. Proliferation of the T cells was analyzed flow cytometrically based on Ki-67 expression or dilution of CellTrace Violet (CTV) after 3 or 5 days of culture as described in the text.

In vitro antibody–mediated protein neutralization

CD11b and PD-L1 were neutralized in vitro using 20 μg/ml of rat anti–mouse/human CD11b (clone M1/70) and 20 μg/ml rat anti–mouse PD-L1 (clone 10F.9G2) (Bio X Cell), respectively. The proteins were added to the culture on set-up days.

Confocal microscopy for live cell imaging

T cells, eosinophils, and DCs were separately labeled with a single-fluorochrome cell surface antibody specific for each population or marker of interest at 20 μl of each antibody per 5 × 10^6 cells in 200 μl of the staining solution containing 2% FBS in PBS. Cells were incubated at 4°C and washed in the staining solution before they were added to the MLR in a 96-well plate as follows: 5 × 10^5 T cells, 5 × 10^5 eosinophils, and 1 × 10^5 DCs (when required). The rat anti-mouse antibodies used include: anti-CD8 FITC (clone 53-6.7) (Thermo Fisher Scientific), anti–Siglec-F PE (clone E50-2440), anti-CD4 Alexa-647 or BV 421 (clone RM4-5), anti-CD11b BV-421 (clone M1/70), and anti-CD11c BV-421 (clone N418) (BD Biosciences). Cells were cultured for 4 hours in the incubator at 37°C and 5% carbon dioxide before the cultures were transferred into the confocal microscope, Operetta CLS (PerkinElmer), where the initial incubation conditions (37°C and 5% carbon dioxide) were also maintained during live cell imaging and data acquisition. Data acquisition and analysis were done with Harmony Software, version 4.5 (PerkinElmer). To analyze eosinophil–T cell or eosinophil-DC contacts, the outer border of each cell population was established and a contact/fluorescence threshold was set after inspection based on the nearness or overlap of cells to one another and measured as the intensity of detection of the fluorochrome signal of 1 cell in another cell type. All cells separated by lower distances than the threshold were captured by the Harmony Software.

Eosinophil ablation

Eosinophils were ablated in iPHIL mice through intraperitoneal administration of DT (MilliporeSigma) as we previously described (15). DT was reconstituted in PBS and administered at a dose of 15 ng/gm of mouse 5, 4, and 3 days before transplantation, and 1 day after transplantation. Control mice received equivalent volume of vehicle.

In vivo antibody-mediated cytokine neutralization

All neutralization antibodies are of rat origin and purchased from Bio X Cell. For the targeted depletion of eosinophils in allograft recipients, 200 μg of anti–mouse/human IL-5 (clone TRFK5) was administered to each mouse 2 days and 1 day before transplantation, and 1 day and 2 days after transplantation.

For the depletion of T cells, 200 μg each of anti–mouse CD4 (clone GK 1.5) and anti–mouse CD8 (clone YTS 169.4) were administered together in a cocktail to each mouse 3 days and 1 day before transplantation, and 1 day after transplantation. Each control animal for all the antibody-mediated cell depletion experiments received an equivalent concentration of rat IgG control (clone HRPN).

In vivo eosinophil mobilization

This was achieved through the intratracheal administration of a combination the following recombinant proteins purchased from Peprotech: 3 μg recombinant mouse CCL11 (eotaxin), 3 μg recombinant mouse CCL24 (eotaxin 2), and 1 μg recombinant mouse IL-5 to each graft recipient immediately after transplant and 1 day after transplant. The chemokine/cytokine combination was given in 100 μl intratracheally.

Quantitative polymerase chain reaction

RNA was extracted from lung digests, and eosinophils were isolated from the lung or in vitro polarized eosinophils using the TRIzol-based technique according to the manufacturer's guidelines (Thermo Fisher Scientific). cDNA was reverse transcribed from RNA samples using the High-Capacity cDNA Reverse Transcription Kit in accordance with the manufacturer's instruction (Thermo Fisher Scientific–Applied Biosystem). Quantitative PCR (qPCR) was performed on the cDNA samples using Power SYBR Green PCR Master Mix (Thermo Fisher Scientific–Applied Biosystem) in a CFX-96 Real-Time PCR Detection System (Bio-Rad). Cycling and reaction conditions were as provided by the manufacturer. The primers used are as follows (FW, forward; RV, reverse): IFN-γ FW: ATGAACGCTACACACTGCATC, RV: CCATCCTTTTGCCAGTTCCTC; TNF-α FW: CCCTCACACTCAGATCATCTTCT, RV: GCTACGACGTGGGCTACAG; IL-5 FW: CTCTGTTGACAAGCAATGAGACG, RV: TCTTCAGTATGTCTAGCCCCTG; IL-33 FW: TCCAACTCCAAGATTTCCCCG, RV: CATGCAGTAGACATGGCAGAA; IL-4 FW: GGTCTCAACCCCCAGCTAGT, RV: GCCGATGATCTCTCTCAAGTGAT; GM-CSF FW: GGCCTTGGAAGCATGTAGAGG, RV: GGAGAACTCGTTAGAGACGACTT; iNOS FW: GTTCTCAGCCCAACAATACAAGA, RV: GTGGACGGGTCGATGTCAC; β-actin FW: CGTGCGTGACATCAAAGAG, RV: TGCCACAGGATTCCATAC; CCL17 FW: TACCATGAGGTCACTTCAGATGC, RV: GCACTCTCGGCCTACATTGG; IL-13 FW: CCTGGCTCTTGCTTGCCTT, RV: GGTCTTGTGTGATGTTGCTCA; CXCL9 FW: GGAGTTCGAGGAACCCTAGTG, RV: GGGATTTGTAGTGGATCGTGC; CXCL10 FW: CCAAGTGCTGCCGTCATTTTC, RV: GGCTCGCAGGGATGATTTCAA; CXCL11 FW: GGCTTCCTTATGTTCAAACAGGG, RV: GCCGTTACTCGGGTAAATTACA; CCL22 FW: AGGTCCCTATGGTGCCAATGT, RV: CGGCAGGATTTTGAGGTCCA.

RNA-Seq gene expression analysis

Sample preparation and RNA extraction. RNA was extracted from $CD8^+$ T cells isolated from left lung allografts of either eosinophil-depleted or -nondepleted B6 recipients of BALB/c left lung grafts 4 days after transplantation, using the TRIzol-based technique according to the manufacturer's guidelines (Thermo Fisher Scientific).

RNA library preparation via polyA selection and multiplexing of Mus musculus. RNA samples were quantified using Qubit 2.0 Fluorometer (Thermo Fisher Scientific–Life Technologies), and RNA integrity was checked with 2100 Bioanalyzer (Agilent Technologies). RNA library preparations, sequencing reactions, and initial bioinformatics analysis were conducted at GENEWIZ, LLC.

RNA sequencing (RNA-Seq) library preparation used the NEBNext Ultra RNA Library Prep Kit for Illumina by following the manufacturer's recommendations (NEB). Briefly, mRNA was first enriched with oligo d(T) beads. Enriched mRNAs were fragmented for 15 minutes at 94°C. First-strand and second-strand cDNA were subsequently synthesized. cDNA fragments were end repaired and adenylated at the 3′ ends, and universal adapter was ligated to cDNA fragments, followed by index addition and library enrichment with limited-cycle PCR. Sequencing libraries were validated using a DNA Chip on the Agilent 2100 Bioanalyzer (Agilent Technologies) and quantified by using Qubit 2.0 Fluorometer (Thermo Fisher Scientific–Invitrogen) as well as by qPCR (Thermo Fisher Scientific–Applied Biosystems).

Sequencing. The sequencing libraries were multiplexed and clustered onto a flow cell. After clustering, the flow cell was loaded on the Illumina HiSeq 4000 or equivalent instrument according to the manufacturer's instructions. The samples were sequenced using a 2 × 150 bp paired-end configuration. Image analysis and base calling were conducted by the HiSeq Control Software (HCS) on the HiSeq instrument. Raw sequence data (.bcl files) generated from Illumina HiSeq were converted into fastq

files and demultiplexed using Illumina bcl2fastq v 2.17 program. One mismatch was allowed for index sequence identification.

RNA-Seq analysis. After investigating the quality of the raw data, sequence reads were trimmed to remove possible adapter sequences and nucleotides with poor quality using Trimmomatic v.0.36. The trimmed reads were mapped to the *Mus musculus* reference genome available on ENSEMBL using the STAR aligner v.2.5.2b. The STAR aligner uses a splice aligner that detects splice junctions and incorporates them to help align the entire read sequences. BAM files were generated as a result of this step. Unique gene hit counts were calculated by using feature counts from the Subread package v.1.5.2. Only unique reads that fell within exon regions were counted. Since a strand-specific library preparation was performed, the reads were strand-specifically counted.

After extraction of gene hit counts, the gene hit counts table was used for downstream differential expression analysis. Using DESeq2, a comparison of gene expression between the groups of samples was performed. The Wald test was used to generate *P* values and $\log_2$ fold changes. Genes with adjusted *P* values less than 0.05 and absolute $\log_2$ fold changes greater than 1 were called as differentially expressed genes for each comparison. A gene ontology (GO) analysis was performed on the statistically significant set of genes by implementing the software GeneSCF. The mgi GO list was used to cluster the set of genes based on their biological process and determine their statistical significance. A PCA analysis was performed using the "plotPCA" function within the DESeq2 R package. The plot shows the samples in a 2D plane spanned by their first 2 principal components. The top 500 genes, selected by highest row variance, were used to generate the plot. The RNA-Seq data have been stored at https://figshare.com/s/e6c0df2faacdf1ffb306. The data can also be located through DOI: 10.6084/m9.figshare.7910444.

Statistics

Friedman's test was used for paired data, while the Kruskall-Wallis test was used for unpaired group of observations. Post hoc analysis of differences and comparison of differences between pairs of data were done with the Wilcoxon rank test and the Mann-Whitney *U* test for paired and unpaired observations, respectively. Differences were considered significant at $P < 0.05$. Differences in RNA-Seq analysis between the test and control groups were further considered significant at an adjusted *P* value < 0.05. The primary outcome measures are presented in scatter or dot plots. For the scatter plots, the inner dark line represents the mean value while the whiskers above and below the mean represent the standard error of mean. For the box plots, the bottom and top of the boxes represent the lower and upper quartiles respectively, the dark band inside the box represents the median, while the top and bottom whiskers represent the maximum and minimum observed values respectively. Data analysis and preparation of figures were done with GraphPad Prism 7.0b software.

Study approval

All animal studies described in this study have been approved by the IACUC of the University of Virginia under protocol numbers 4148 (approved on 12/6/16) and 4149 (approved on 12/6/16) or Mayo Clinic in Arizona under protocol number A00004152-18 (approved on 12/14/2018) and IACUC number A00002950-17 (approved on 7/19/2017). No human subjects or tissue were utilized in this work.

Author contributions

OOO managed and organized the studies, conducted the immunology and cell biology experiments, bred animals, analyzed data, and wrote the manuscript. YG conducted and coordinated the animal surgeries. BM assisted with the immunology experiments. AM and ZM assisted with the animal surgeries. MHS did the pathological scoring of the tissue slides for rejection grading. QW, AB, DL, MTZ, and AGS assisted with some critical experiments. DK and AEG helped write the manuscript and assisted with the study concept design. EAJ and ASK designed the study, performed experiments, analyzed data, and wrote the manuscript.

Acknowledgments

ASK is supported by NIH grants P01 AI116501, R41 CA224520-01, IBX004588A, and R01 AI145108-01. EAJ is supported by NIH grants R01 AI145108-01, R01 HL065228, R01 HL124165, R21 AI132840, UG1HL139504-1, and the Mayo Clinic Foundation. We appreciate the technical support we received from Joanne Lannigan, Flow Cytometry Core Facility, University of Virginia, Charlottesville, Virginia, USA;

Stacey Criswell, Advanced Microscopy Core Facility, University of Virginia, Charlottesville, Virginia, USA; and Catherine Ulich, PerkinElmer, Boston, Massachusetts, USA.

Address correspondence to: Alexander Krupnick, Professor of Surgery, Department of Surgery and Carter Immunology Center, University of Virginia, P.O. Box 800679, Charlottesville, Virginia 22908, USA. Phone: 434.924.8016; Email: sashak@virginia.edu.

1. Balsara KR, et al. A single-center experience of 1500 lung transplant patients. *J Thorac Cardiovasc Surg*. 2018;156(2):894–905.e3.
2. Kulkarni HS, et al. Bronchiolitis obliterans syndrome-free survival after lung transplantation: An International Society for Heart and Lung Transplantation Thoracic Transplant Registry analysis. *J Heart Lung Transplant*. 2019;38(1):5–16.
3. Witt CA, Puri V, Gelman AE, Krupnick AS, Kreisel D. Lung transplant immunosuppression — time for a new approach? *Expert Rev Clin Immunol*. 2014;10(11):1419–1421.
4. Knoop C, Haverich A, Fischer S. Immunosuppressive therapy after human lung transplantation. *Eur Respir J*. 2004;23(1):159–171.
5. Krupnick AS, et al. Central memory $CD8^+$ T lymphocytes mediate lung allograft acceptance. *J Clin Invest*. 2014;124(3):1130–1143.
6. Schenk AD, Nozaki T, Rabant M, Valujskikh A, Fairchild RL. Donor-reactive CD8 memory T cells infiltrate cardiac allografts within 24-h posttransplant in naive recipients. *Am J Transplant*. 2008;8(8):1652–1661.
7. Onyema OO, et al. Eosinophils promote inducible NOS-mediated lung allograft acceptance. *JCI Insight*. 2017;2(24):96455.
8. Goldman M, Le Moine A, Braun M, Flamand V, Abramowicz D. A role for eosinophils in transplant rejection. *Trends Immunol*. 2001;22(5):247–251.
9. Jacobsen EA, et al. Differential activation of airway eosinophils induces IL-13-mediated allergic Th2 pulmonary responses in mice. *Allergy*. 2015;70(9):1148–1159.
10. Abdala-Valencia H, et al. Shaping eosinophil identity in the tissue contexts of development, homeostasis, and disease. *J Leukoc Biol*. 2018;104(1):95–108.
11. Kato T, Nariuchi H. Polarization of naive $CD4^+$ T cells toward the Th1 subset by CTLA-4 costimulation. *J Immunol*. 2000;164(7):3554–3562.
12. Sharpe AH. Mechanisms of costimulation. *Immunol Rev*. 2009;229(1):5–11.
13. Markey KA, et al. Cross-dressing by donor dendritic cells after allogeneic bone marrow transplantation contributes to formation of the immunological synapse and maximizes responses to indirectly presented antigen. *J Immunol*. 2014;192(11):5426–5433.
14. Mesnil C, et al. Lung-resident eosinophils represent a distinct regulatory eosinophil subset. *J Clin Invest*. 2016;126(9):3279–3295.
15. Jacobsen EA, et al. Eosinophil activities modulate the immune/inflammatory character of allergic respiratory responses in mice. *Allergy*. 2014;69(3):315–327.
16. Murphy MP. Nitric oxide and cell death. *Biochim Biophys Acta*. 1999;1411(2–3):401–414.
17. Schouppe E, Van Overmeire E, Laoui D, Keirsse J, Van Ginderachter JA. Modulation of CD8(+) T-cell activation events by monocytic and granulocytic myeloid-derived suppressor cells. *Immunobiology*. 2013;218(11):1385–1391.
18. Nagaraj S, et al. Altered recognition of antigen is a mechanism of $CD8^+$ T cell tolerance in cancer. *Nat Med*. 2007;13(7):828–835.
19. Nagaraj S, Schrum AG, Cho HI, Celis E, Gabrilovich DI. Mechanism of T cell tolerance induced by myeloid-derived suppressor cells. *J Immunol*. 2010;184(6):3106–3116.
20. Ashouri JF, Weiss A. Endogenous Nur77 is a specific indicator of antigen receptor signaling in human T and B cells. *J Immunol*. 2017;198(2):657–668.
21. Moran AE, et al. T cell receptor signal strength in Treg and iNKT cell development demonstrated by a novel fluorescent reporter mouse. *J Exp Med*. 2011;208(6):1279–1289.
22. Schrum AG, et al. High-sensitivity detection and quantitative analysis of native protein-protein interactions and multiprotein complexes by flow cytometry. *Sci STKE*. 2007;2007(389):pl2.
23. Gelman AE, et al. Cutting edge: Acute lung allograft rejection is independent of secondary lymphoid organs. *J Immunol*. 2009;182(7):3969–3973.
24. Jacobsen EA, Zellner KR, Colbert D, Lee NA, Lee JJ. Eosinophils regulate dendritic cells and Th2 pulmonary immune responses following allergen provocation. *J Immunol*. 2011;187(11):6059–6068.
25. Veres TZ, et al. Allergen-induced $CD4^+$ T cell cytokine production within airway mucosal dendritic cell-T cell clusters drives the local recruitment of myeloid effector cells. *J Immunol*. 2017;198(2):895–907.
26. Pillay J, et al. A subset of neutrophils in human systemic inflammation inhibits T cell responses through Mac-1. *J Clin Invest*. 2012;122(1):327–336.
27. Takahashi T, et al. PD-1 expression on $CD8^+$ T cells regulates their differentiation within lung allografts and is critical for tolerance induction. *Am J Transplant*. 2018;18(1):216–225.
28. Lotfi R, Lotze MT. Eosinophils induce DC maturation, regulating immunity. *J Leukoc Biol*. 2008;83(3):456–460.
29. Rankin SM, Conroy DM, Williams TJ. Eotaxin and eosinophil recruitment: implications for human disease. *Mol Med Today*. 2000;6(1):20–27.
30. Shen ZJ, Malter JS. Determinants of eosinophil survival and apoptotic cell death. *Apoptosis*. 2015;20(2):224–234.
31. Jacobsen EA, et al. Allergic pulmonary inflammation in mice is dependent on eosinophil-induced recruitment of effector T cells. *J Exp Med*. 2008;205(3):699–710.
32. Lilly LM, Scopel M, Nelson MP, Burg AR, Dunaway CW, Steele C. Eosinophil deficiency compromises lung defense against Aspergillus fumigatus. *Infect Immun*. 2014;82(3):1315–1325.
33. Hagan P, Wilkins HA, Blumenthal UJ, Hayes RJ, Greenwood BM. Eosinophilia and resistance to Schistosoma haematobium in man. *Parasite Immunol*. 1985;7(6):625–632.
34. Jacobsen EA, Lee NA, Lee JJ. Re-defining the unique roles for eosinophils in allergic respiratory inflammation. *Clin Exp Allergy*. 2014;44(9):1119–1136.

35. Nagral A, Ben-Ari Z, Dhillon AP, Burroughs AK. Eosinophils in acute cellular rejection in liver allografts. *Liver Transpl Surg*. 1998;4(5):355–362.
36. Arbon KS, Albers E, Kemna M, Law S, Law Y. Eosinophil count, allergies, and rejection in pediatric heart transplant recipients. *J Heart Lung Transplant*. 2015;34(8):1103–1111.
37. Arnold IC, et al. Eosinophils suppress Th1 responses and restrict bacterially induced gastrointestinal inflammation. *J Exp Med*. 2018;215(8):2055–2072.
38. Miller ML, et al. Distinct graft-specific TCR avidity profiles during acute rejection and tolerance. *Cell Rep*. 2018;24(8):2112–2126.
39. Pardoll DM. The blockade of immune checkpoints in cancer immunotherapy. *Nat Rev Cancer*. 2012;12(4):252–264.
40. Tanaka K, et al. PDL1 is required for peripheral transplantation tolerance and protection from chronic allograft rejection. *J Immunol*. 2007;179(8):5204–5210.
41. Patsoukis N, Brown J, Petkova V, Liu F, Li L, Boussiotis VA. Selective effects of PD-1 on Akt and Ras pathways regulate molecular components of the cell cycle and inhibit T cell proliferation. *Sci Signal*. 2012;5(230):ra46.
42. Goldman N, et al. High macrophage PD-L1 expression not responsible for T cell suppression. *Cell Immunol*. 2018;324:50–58.
43. Deuse T, et al. Mechanisms behind local immunosuppression using inhaled tacrolimus in preclinical models of lung transplantation. *Am J Respir Cell Mol Biol*. 2010;43(4):403–412.
44. Groves S, et al. Inhaled cyclosporine and pulmonary function in lung transplant recipients. *J Aerosol Med Pulm Drug Deliv*. 2010;23(1):31–39.
45. Lee NA, McGarry MP, Larson KA, Horton MA, Kristensen AB, Lee JJ. Expression of IL-5 in thymocytes/T cells leads to the development of a massive eosinophilia, extramedullary eosinophilopoiesis, and unique histopathologies. *J Immunol*. 1997;158(3):1332–1344.
46. Okazaki M, et al. A mouse model of orthotopic vascularized aerated lung transplantation. *Am J Transplant*. 2007;7(6):1672–1679.
47. Krupnick AS, et al. Orthotopic mouse lung transplantation as experimental methodology to study transplant and tumor biology. *Nat Protoc*. 2009;4(1):86–93.
48. Larsen CP, et al. Long-term acceptance of skin and cardiac allografts after blocking CD40 and CD28 pathways. *Nature*. 1996;381(6581):434–438.
49. Yousem SA, et al. Revision of the 1990 working formulation for the classification of pulmonary allograft rejection: Lung Rejection Study Group. *J Heart Lung Transplant*. 1996;15(1 pt 1):1–15.
50. Bradshaw KN, Weng-Race J, Ward JM, Rehg JE, Kovacs JA, Davis AS. Reliable CD4 and CD8 T cell marker immunohistochemistry on formalin-fixed and histochoice-fixed paraffin embedded mouse spleen. *FASEB J*. 2017;31(1_supplement):979.5.
51. Jacobsen EA, et al. Lung pathologies in a chronic inflammation mouse model are independent of eosinophil degranulation. *Am J Respir Crit Care Med*. 2017;195(10):1321–1332.
52. Wabnitz GH, et al. L-plastin phosphorylation: a novel target for the immunosuppressive drug dexamethasone in primary human T cells. *Eur J Immunol*. 2011;41(11):3157–3169.
53. Helft J, et al. GM-CSF mouse bone marrow cultures comprise a heterogeneous population of CD11c(+)MHCII(+) macrophages and dendritic cells. *Immunity*. 2015;42(6):1197–1211.